



Semnan University

Mechanics of Advanced Composite Structures

journal homepage: <http://MACS.journals.semnan.ac.ir>

Analytical and Numerical Solution of Heat Transfer Equation in Rectangular Composite Fins

M. Hajinejad Sorkhi, Y. Rostamiyan *

Department of Mechanical Engineering, Islamic Azad University of Sari, Iran.

KEYWORDS

Differential transform method;
Numerical solution;
Exact solution;
FEM solution.

ABSTRACT

Today, the use of composites has received widespread attention due to their special properties that cannot be found in alloys. Kevlar-Epoxy composite is one of the most widely used materials. In this paper, we analyze the heat transfer in rectangular fin and present an exact, Differential Transform Method and FEM solution for steady-state conduction heat transfer in rectangular composite laminates. The differential Transformation Method (DTM), is applied for predicting the temperature distribution in a rectangular composite fin. Laminate with fiber orientations of 0° is considered for the analysis. By validating the results in one composite layer, the temperature changes and heat flux in several composite layers were finally simulated in ABAQUS software and the effect of the number of composite layers and time on these parameters have been investigated. The selected composite fin's material is Kevlar-epoxy. The results show that the exact solution and DTM predict the same trend compared to the FEM result and are very accurate and there is a good match between FEM results with DTM method and the exact solution. The thermo-geometric fin parameter (μ), the number of composite layers, and time have a significant effect on temperature distribution and heat flux. By increasing of thermo-geometric fin parameter (μ), heat flux and dimensionless variable for temperature distribution increase. When the number of layers increases, the dimensionless variable for temperature distribution and heat flux decrease along the fin. With increasing time, the temperature distribution and heat flux become more uniform and the ratio of heat flux changes decreases along the fin.

1. Introduction

Today, the use of composites has received widespread attention due to their special properties that cannot be found in alloys. The use of composites has been widely used due to their special properties that cannot be found in alloys. One way to improve the mechanical properties of composites is to produce multi-layered sheets [1]. Today, the use of composite materials for the production of equipment, machinery, and structures has expanded dramatically. With composite, the weight of materials, structures, and costs are reduced. In some industries, the use of these materials is unique compared to isotropic materials. Scientific works usually end with the behavior of these mechanical and thermal loads, and we rarely see other effects such as heat transfer in this category of materials. Scientific works usually include the behavior of

these mechanical and thermal loads, and we rarely see other effects such as heat transfer in this category of materials.

One of the most important applications of heat transfer in composite materials is the manufacturing process, which includes cooking, cutting and welding fiber, and so on. Preliminary work in this area is based on one-dimensional heat transfer in heterogeneous crystals [2, 3]. Fins are surfaces that have an initial material that flows into a liquid around them. They are used mainly for heat transfer rates between the body and the surrounding environment. Their outer surface is designed to increase the level of an object and cause the conditions to be identical to the environment. Argyris et al. [4] analytically studied heat transfer in flat laminates they have made a triangle. They considered the influence of the formulation of all three mechanisms of conduction, convection, and radiant heat transfer

* Corresponding author. Tel.: +98-9111537063
E-mail address: yasser.rostamiyan@iausari.ac.ir

of laminate flooring. We [5-6] proposed an analytical solution of conductive heat transfer in colleagues non-radioisotope multilayer environments in two modes, without doors by considering the heat source and the internal heating, respectively. They have been examined separately. They use a conversion of the linear coordinates to transform the anisotropic problem to simply isotropic. They have changed and solved the problem. Gou [7] investigated numerical conduction heat transfer in laminates. In this study the thickness and using the finite element method, on-permanent heat transfer in the presence of domestic energy production has been checked. The Differential Transformation Method is used to solve some problems. The method was successfully applied to various application problems.

Recently, this kind of problem has been analyzed by some researchers using different methods. Carly and Advani [8] studied the temperature of a thin composite plate that is exposed to a central heating source with numerical methods and they have gained experience. They did a parametric study to determine the important dimensionless numbers and their effect on temperature distribution. Yaziciog et al. [9] studied the optimum fin spacing of rectangular fins on a vertical base in free convection heat transfer. The separate roles of fin height, fin spacing, and base to ambient temperature difference were investigated. It was found that for a given base to ambient temperature difference, the convective heat transfer rate from fin arrays takes on a maximum value as a function of fin spacing and fin height and an optimum fin spacing value which maximizes the convective heat transfer rate from the fin array is available for every fin height.

Dialameh et al. [10] analyzed natural convection from an array of horizontal rectangular thick fins with short length. In this article, a numerical study is made to predict natural convection from an array of aluminum horizontal rectangular thick fins of $3 \text{ mm} < t < 7 \text{ mm}$ with short lengths ($L \leq 50 \text{ mm}$) attached to a horizontal base plate. The three-dimensional elliptic governing equations of laminar flow and heat transfer were solved using finite volume scheme. For 128 fin geometries. Joneidi et al. [11] studied the fin efficiency of convective straight fins with temperature-dependent thermal conductivity is solved using a simulation method called the Differential Transformation Method (DTM). They analyzed the effects of some physical applicable parameters in this problem such as thermo-geometric fin parameter and thermal conductivity parameter.

Naidu et al. [12] studied natural convection heat transfer from fin arrays in experimental and

theoretical studies on the effect of inclination of base on heat transfer. Numerical results are obtained for temperature along the length of the fin and in the fluid in the enclosure. The experimental studies have been also carried out on two geometric orientations, (a) vertical base with vertical fins (vertical fin array) and (b) horizontal base with vertical fins (horizontal fin array), with the five different inclinations like 00, 300, 450, 600, and 900. The experimental results are compared with the numerical results computed by the theoretical analysis and show good agreement.

Tanigawa et al. [13] conducted thermal bending analysis of a laminated composite rectangular plate due to a partially distributed heat supply. They examined the effect of relaxation on distributions of the thermal stress and thermal deflection for the nonhomogeneous rectangular plate. Tari et al. [14] investigated the natural convection and radiation heat transfer from eleven large vertically based fin arrays. In the former work.

Hatami et al. [15] studied heat transfer through porous fins (Si_3N_4 and AL) with temperature-dependent heat generation. Three highly accurate and simple analytical methods, Differential Transformation Method (DTM), Collocation Method (CM), and Least Square Method (LS) are applied for predicting the temperature distribution in a porous fin with temperature dependent internal heat generation. Their results could indicate that the temperature distribution is strongly dependent on the Darcy and Rayleigh numbers and a higher heat generation rate leads to higher fin temperatures since more amount of heat is dissipated to the surrounding.

Ahmadi et al. [16] studied effect of interrupted fins in heat transfer in external natural convection is studied. Provision of interruption length ranging from 20mm to 40mm with a variable number of interruptions ranging from 2 to 4 is investigated. Results are more prominent towards optimized parameters i.e. number of interruptions and interruption length. Jacob et al. [17] studied the optimization of triangular fins. Their optimization provided general guidelines relative to the dimensionless characteristics of a well-designed fin.

Bunjaku et al. [18] analyzed geometric parameters of rectangular and triangular fins with Constant surfacing. They reported the optimal geometrical parameters of the fins might serve as a practical tool for engineers involved in designing of fined heat transfer surfaces. Gupta et al. [19] studied analytical thermal analysis on straight triangular fins. They reported base wall temperature, total area for heat convection, heat dissipation rate, fin efficiency, fin effectiveness,

and contours of temperature distribution and heat flux.

Fallo et al. [20] provide predictions for the transfer of composite materials. It is mainly limited to numerical opinions and arguments. Namdari et al. [21] analyzed numerical solutions for transient heat transfer in longitudinal fins. They reported that the parabolic fin has the lowest rate of heat transfer while the rectangular and convex profiles have the highest rate of heat transfer respectively. Pasha et al. [22] presented an analysis of unsteady heat transfer of specific longitudinal fins with Temperature-dependent thermal coefficients by DTM. In this paper, it has been shown that DTM is a very useful method to solve these problems when e and M are increasing the temperature plot going to the lower level so efficiencies are being lowered.

Patel et al. [23] investigated comparative thermal analysis of Fins the models were designed in ANSYS. The fins were analyzed for forced convection. The fins were compared based on non-dimensional Nusselt number and Reynolds number. Mazhar et al. [24] studied numerical analysis of rectangular fins in a PCM for low-grade heat harnessing. Compared to a non-finned geometry this optimized fin configuration enhances the effective thermal conductivity of the PCM by a factor of 1.38 for melting and 4.75 for freezing. Their results showed The GW to CW energy transfer efficiency is 72.4% with higher fluid flow temperature increments, compared to only 47.3% for a non-finned version. Adhikari et al. [25] had an experimental and numerical study of forced convection heat transfer from rectangular fins at low Reynolds numbers. Their results showed that heat transfer rate per channel decreases linearly with the increase in channel length, but remains approximately constant with the increase in the number of fins.

Past research studies show that it is very important to study the heat transfer and effective parameters on heat transfer in the fins. Also, due to the special properties of composite materials, the study of these parameters in composite fins is an important problem and issue that should be considered. Based on the authors' knowledge, the thermo-geometric fin parameter (μ), the number of the composite layers, and time on heat transfer, temperature distribution, and heat flux in Kevlar-epoxy rectangular composite fin have not been investigated with a combination of three methods of analytical, DTM and FEM.

We use Kevlar-Epoxy composite in this research because Kevlar is a conductive material and epoxy is a heat insulator and is a significant difference between conductive heat transfer coefficient in fibers and matrix materials. Heat transfer analysis in this composite can help us to

understand heat transfer in composite materials. Also, using DTM method in solving these problems is very accurate. Therefore, in this paper, the effect of important parameters on the heat transfer of composite fin was investigated using FEM, DTM, and analytical methods. The present solution can be done in many operations applications to calculate temperature distributions and heat flux to be useful.

2. Heat conduction in composites

Fourier equation for conductive heat transfer in orthotropic materials can be expressed as follows [26]:

$$\begin{pmatrix} q_x \\ q_y \\ q_z \end{pmatrix} = - \begin{bmatrix} k_{11} & k_{12} & k_{13} \\ k_{21} & k_{22} & k_{23} \\ k_{31} & k_{32} & k_{33} \end{bmatrix} \begin{Bmatrix} \frac{\partial T}{\partial x} \\ \frac{\partial T}{\partial y} \\ \frac{\partial T}{\partial z} \end{Bmatrix} \quad (1)$$

k_{ij} is Conductive heat transfer coefficients and q , heat flux and T is temperature. Due to the Onsager reciprocity, the tensor of conductive heat transfer coefficients, for all substances in nature must be symmetric [27]:

$$k_{ij} = k_{ji} \quad (2)$$

According to the second law of thermodynamics, the diametric elements of this tensor are positive and the following relation must be established [28]:

$$k_{ij}k_{jj} > k_{ij}^2 \quad \text{for: } i \neq j \quad (3)$$

Due to the Clausius-Duhem relationship, the following inequalities are managed between the orthotropic material conductance coefficients [26, 28, and 29]:

$$k_{ii} \geq 0 \quad (4)$$

$$\frac{1}{2}(k_{ii}k_{jj} - k_{ij}k_{ji}) \geq 0 \quad (5)$$

$$\epsilon_{ijk} k_{1j}k_{2j}k_{3j} \geq 0 \quad (6)$$

where, k_{ij} introduces symmetric part of conductivity tensor:

$$k_{ij} = k_{ji} = \frac{k_{ij} + k_{ji}}{2} \quad (7)$$

According to the problem, two different coordinate systems are defined: on-axis (X_1, X_2 and X_3) and off-axis (X, Y , and Z) [30]. As shown in Fig1, the direction of on-axis coordinates depends on fiber orientation, in a way that x_1 is in the direction of the fibers, X_2 is perpendicular to X_1 in the composite layers and X_3 is perpendicular to the layer plane. To study physical properties, we must also define an out-of-axis reference coordinate system. Also, there is an angular deviation by h between the on-axis and off-axis system and these coordinates are coincident.

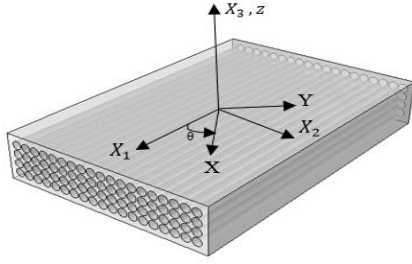


Fig. 1. On-axis and off-axis coordinate systems

In the on-axis coordinate system, the Fourier relation for a composite material can be expressed as follows [31]:

$$\begin{Bmatrix} q_1 \\ q_2 \\ q_3 \end{Bmatrix}_{on} = - \begin{bmatrix} k_{11} & 0 & 0 \\ 0 & k_{22} & 0 \\ 0 & 0 & k_{22} \end{bmatrix} \begin{Bmatrix} \frac{\partial T}{\partial x} \\ \frac{\partial T}{\partial y} \\ \frac{\partial T}{\partial z} \end{Bmatrix}_{on} \quad (8)$$

Because of Eq. 8, properties in direction of fibers (X_1) is different from those in perpendicular directions (X_2, X_3) in each lamina. But in the perpendicular plane to the fibers, heat transfers in all directions are the same. With a rotation of the on-axis system by $(-\theta)$, Eq. 8 can be obtained in the off-axis system:

$$[T(-\theta)]\{q\}_{off} = -[k]_{on}[T(-\theta)]\nabla T_{off} \quad (9)$$

$T(\theta)$ is the rotation sensor conversion shown in Equation 9 is obtained from the following equation:

$$[T(\theta)] = - \begin{bmatrix} \cos \theta & -\sin \theta & 0 \\ \sin \theta & \cos \theta & 0 \\ 0 & 0 & 1 \end{bmatrix} \begin{Bmatrix} \frac{\partial T}{\partial x} \\ \frac{\partial T}{\partial y} \\ \frac{\partial T}{\partial z} \end{Bmatrix} \quad (10)$$

Also, the heat flux in the off-axis directions using Equation 10 is as follows:

$$\{q\}_{off} = -[T(-\theta)]^{-1}[k]_{on}[T(-\theta)]\nabla T_{off} \quad (11)$$

Given that the rotary torque converter is orthogonal, it can be written:

$$[T(-\theta)]^{-1} = [T(-\theta)] \quad (12)$$

To calculate the heat flux vector in the off-axis directions, it is sufficient to replace Equation 12 with Equation 11.

$$\{Q\}_{off} = -[T(\theta)][k]_{on}[T(-\theta)]\nabla T_{off} \quad (13)$$

According to Fourier law, heat flux in off-axis directions is:

$$\{q\}_{off} = -[k]_{off} \nabla T_{off} \quad (14)$$

Then, in order to obtain the off-axis heat transfer coefficient tensor in terms of on-axis coordinate system was compared with the comparison of equations 13 and 14:

$$[k]_{off} = [T(\theta)][k]_{on}[T(-\theta)] \quad (15)$$

The heat transfer coefficient tensor in on-axis system and off-axis system are shown by $[k]$ and $[\bar{k}]$, respectively, and $\cos \theta$ is shown by m_1 and $\sin \theta$ by n_1 , equations 8, 10, and 15 can be used to obtain the tensor elements of heat transfer coefficient in off-axis directions:

$$\bar{k}_{11} = m_1^2 k_{11} + n_1^2 k_{22} \quad (16)$$

$$\bar{k}_{22} = n_1^2 k_{11} + m_1^2 k_{22} \quad (17)$$

$$\bar{k}_{33} = k_{22} \quad (18)$$

$$\bar{k}_{12} = \bar{k}_{21} = m_1 n_1 (k_{11} - k_{22}) \quad (19)$$

$$\bar{k}_{13} = \bar{k}_{31} = 0 \quad (20)$$

$$\bar{k}_{23} = \bar{k}_{32} = 0 \quad (21)$$

The following relationships have been used to calculate the conduction coefficients (k_{11}, k_{22}) in on-axis system. This method is a suitable method with

An error of less than 2% the lack of laboratory facilities is very helpful. Equations 22-25 can be generalized to other physical properties of the composite materials. [32]:

$$k_{11} = v_f k_f + v_m k_m \quad (22)$$

$$k_{22} = k_m \frac{1 + \xi \eta v_f}{1 - \eta v_f} \quad (23)$$

In equations 22 and 23 k_f is a Fiber thermal conductivity coefficient, k_m is the Thermal conductivity coefficient of the ground material, v_f is the volumetric percentage of fiber, v_m and is the volume percentage of the material is background. Quantities η and ξ are also calculated from the following equations:

$$\eta = \frac{\frac{k_f}{k_m} - 1}{\frac{k_f}{k_m} + \xi} \quad (24)$$

$$\xi = \frac{1}{4 - 3v_m} \quad (25)$$

2.1. Modeling and formulations

Figure 2 shows steady-state heat transfer in a composite rectangular fin in this research. Figure 2 shows the direction of the fibers in specific directions in the rectangle composite. The Fourier relation in a rectangular coordinate system for orthotropic material is given below [26]:

$$\begin{Bmatrix} q_x \\ q_y \\ q_z \end{Bmatrix} = - \begin{bmatrix} \bar{k}_{11} & \bar{k}_{12} & \bar{k}_{13} \\ \bar{k}_{21} & \bar{k}_{22} & \bar{k}_{23} \\ \bar{k}_{31} & \bar{k}_{32} & \bar{k}_{33} \end{bmatrix} \begin{Bmatrix} \frac{\partial T}{\partial x} \\ \frac{\partial T}{\partial y} \\ \frac{\partial T}{\partial z} \end{Bmatrix} \quad (26)$$

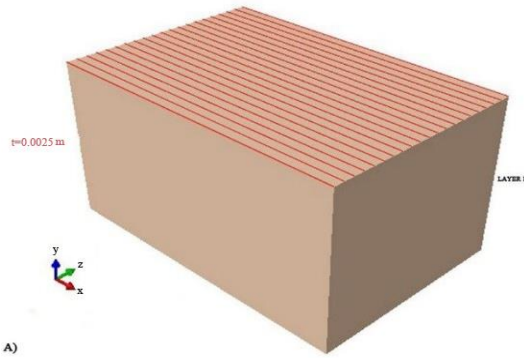


Fig. 2. The fibers' direction in a rectangular laminate

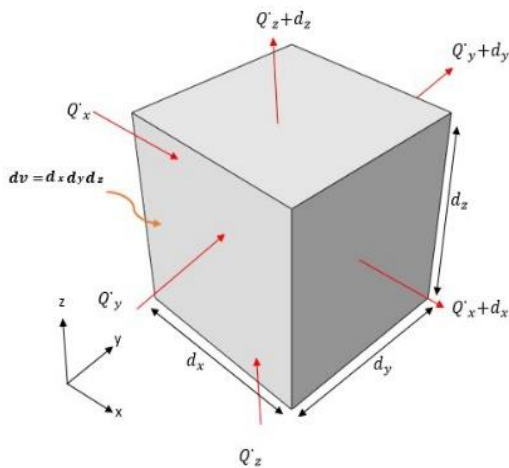


Fig. 3. Heat fluxes in a rectangular element

In Fig. 3 if the energy balance for the element a rectangular is formed, the result is as follows:

$$\rho c \frac{\partial T}{\partial t} dv = - \frac{\partial q_x dA_x}{\partial x} dx - \frac{\partial q_y dA_y}{\partial y} dy - \frac{\partial q_z dA_z}{\partial z} dz \quad (27)$$

In equation (27), C specific heat capacity, ρ density, time, and the V is volume. Also, the values of the size of the surfaces and Elements are:

$$dA_x = dydz \quad (28)$$

$$dA_y = dx dz \quad (29)$$

$$dA_z = dx dy \quad (30)$$

$$dv = dx dy dz \quad (31)$$

By applying equations (26) and (28-31) in equation (27), the heat transfer relationship is obtained for the orthotropic material [33] to [36]:

$$\rho c \frac{\partial T}{\partial t} dx dy dz = - \frac{\partial q_x dy dz}{\partial x} dx - \frac{\partial q_y dx dz}{\partial y} dy - \frac{\partial q_z dx dy}{\partial z} dz \quad (32)$$

$$\frac{\partial \left(\overline{k_{11}} \frac{\partial T}{\partial x} + \overline{k_{12}} \frac{\partial T}{\partial y} \right)}{\partial x} + \frac{\partial \left(\overline{k_{12}} \frac{\partial T}{\partial x} + \overline{k_{22}} \frac{\partial T}{\partial y} \right)}{\partial y} \quad (33)$$

$$+ \frac{\partial \left(\overline{k_{22}} \frac{\partial T}{\partial z} \right)}{\partial z} = \rho c \frac{\partial T}{\partial t} \quad (34)$$

$$\overline{k_{11}} \frac{\partial^2 T}{\partial x^2} + \overline{k_{22}} \frac{\partial^2 T}{\partial y^2} + 2\overline{k_{12}} \frac{\partial^2 T}{\partial x \partial y} + \overline{k_{33}} \frac{\partial^2 T}{\partial z^2} = \rho c \frac{\partial T}{\partial t}$$

$$\left(m_1^2 k_{11} + n_1^2 k_{22} \right) \frac{\partial^2 T}{\partial x^2} + \left(n_1^2 k_{11} + m_1^2 k_{22} \right) \frac{\partial^2 T}{\partial y^2} + 2m_1 n_1 (k_{11} - k_{22}) \frac{\partial^2 T}{\partial x \partial y} + k_{22} \frac{\partial^2 T}{\partial z^2} = \rho c \frac{\partial T}{\partial t} \quad (35)$$

In steady state, the time derivative term on the right the relation (35) is equal to zero. And the end temperature of the fin is also constant. Also, the derivative of temperature changes at the beginning of the fin is considered zero. And the temperature at the boundary of each layer is equal. In this study, such conditions are considered for the rectangular Taken. Figure 4 shows the layers in rectangular laminate i and i + 1 are the boundaries between the two layers in this thickness.

$$T^i = T^{i+1} \quad (36)$$

$$(T - T_\infty)_{x=L} = (T_L - T_\infty) \quad (37)$$

$$\frac{d}{dx} (T - T_\infty) |_{x=0} = 0 \quad (38)$$

$$\dot{q}A = Ph(T - T_\infty)dx + (\dot{q}A + \frac{d\dot{q}}{dx} dx A) \quad (39)$$

By applying the (36-39) conditions, equation 35 is simplified as follows:

$$\left(m_1^2 k_{11} + n_1^2 k_{22} \right) \frac{d^2 T}{dx^2} - \frac{Ph}{A} (T - T_\infty) = 0 \quad (40)$$

In relation, h is the external heat transfer coefficient ($\frac{W}{m^2K}$), p is a rectangular fin perimeter (m) and A is the cross-sectional area of the fin (m²).

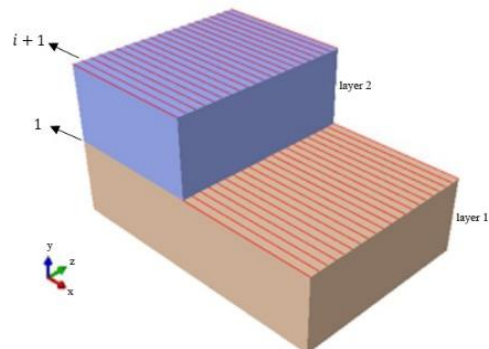


Fig. 4. Layers arrangement in a rectangular laminate

3. Exact solution

The energy balance for a rectangular element in Fig. 3 can be written in terms of the heat flux, for a fin of constant area [40]:

$$\dot{Q} = q \cdot A \tag{41}$$

$$q \cdot A = Ph(T - T_{\infty})dx + \left(\dot{q}A + \frac{d\dot{q}}{dx} dx A \right) \tag{42}$$

$$A \frac{d\dot{q}}{dx} + Ph(T - T_{\infty}) = 0 \tag{43}$$

$$(m_1^2 k_{11} + n_1^2 k_{22}) \frac{\partial^2 T}{\partial x^2} - \frac{Ph}{A} (T - T_{\infty}) = 0 \tag{44}$$

$$(m_1^2 k_{11} + n_1^2 k_{22}) = \epsilon \tag{45}$$

$$\frac{d^2 T}{dx^2} - \frac{Ph}{\epsilon A} (T - T_{\infty}) = 0 \tag{46}$$

$$A \frac{d\dot{q}}{dx} + Ph(T - T_{\infty}) = 0 \tag{47}$$

$$(m_1^2 k_{11} + n_1^2 k_{22}) \frac{\partial^2 T}{\partial x^2} - \frac{Ph}{A} (T - T_{\infty}) = 0 \tag{48}$$

$\theta = \frac{(T - T_{\infty})}{(T_1 - T_{\infty})}$ is a dimensionless variable for temperature difference, and we can change variables to put:

$$\frac{dT}{dx} = \frac{d}{dx} (T - T_{\infty}) \tag{49}$$

$$\frac{\frac{(T - T_{\infty})}{(T_1 - T_{\infty})}}{dx} = \frac{d\theta}{dx} \tag{50}$$

$$\frac{d^2 \theta}{dx^2} - \left(\frac{Ph}{\epsilon A} \right) \theta = 0 \tag{51}$$

$$(T - T_{\infty})_{x=l} = T_l - T_{\infty} \tag{52}$$

$$\frac{d}{dx} (T - T_{\infty})|_{x=0} = 0 \tag{53}$$

where the values of θ range from 0 to 1 and $\lambda = x/L$, where λ also ranges from zero to one. The relation between derivatives that is needed to cast the equation in terms of λ is:

$$\frac{d}{dx} = \frac{d \, d\lambda}{d\lambda \, dx} = \frac{1}{L} \frac{d}{d\lambda} \tag{54}$$

Equation (51) can be written dimensionless.

$$\frac{d^2 \theta}{d\lambda^2} - \left(\frac{Ph}{\epsilon A} L^2 \right) \theta = 0 \tag{55}$$

There is one non-dimensional parameter in Equation (55), which we will call μ and define by:

$$\mu = \left(\frac{Ph}{\epsilon A} L^2 \right)^{\frac{1}{2}} \tag{56}$$

The equation for the temperature distribution, we have obtained is:

$$\frac{d^2 \theta}{d\lambda^2} - \mu^2 \theta = 0 \tag{57}$$

$$\theta = ae^{\mu\lambda} + b e^{-\mu\lambda} \tag{58}$$

The boundary condition at $\lambda = 0$ is:

$$\frac{d\theta}{d\lambda}(0) = \mu a e^0 - \mu b e^0 = 0 \tag{59}$$

$$\mu a - \mu b = 0 \tag{60}$$

The boundary condition at $\lambda = 1$ is:

$$\theta(1) = ae^{\mu} + b e^{-\mu} = 1 \tag{61}$$

$$ae^{\mu} + b e^{-\mu} = 1 \tag{62}$$

4. Differential transformation method

4.1. Principles of method

The Differential Transformation Method is a method that can be used to find the expansion of Taylor from differential equations. It is assumed that $x(t)$, the analytical function in domain D and $(t - t_i)$ represents any point within this domain it is written as a series of powers around point $x(t)$. The extension of the Taylor series of its function is as follows:

$$x(t) = \sum_{k=0}^{\infty} \frac{(t - t_i)^k}{k!} \left[\frac{d^k x(t)}{dt^k} \right]_{t=t_i} \quad \forall t \in D \tag{61}$$

For calculation, the McLaurin series of $x(t)$ can be obtained by taking $t_i = 0$ in equation (61) expressed as [11]:

$$x(t) = \sum_{k=0}^{\infty} \frac{t^k}{k!} \left[\frac{d^k x(t)}{dt^k} \right]_{t=0} \quad \forall t \in D \tag{62}$$

As explained in [37] the differential transformation of the function $x(t)$ is defined as follows:

$$x(k) = \sum_{k=0}^{\infty} \frac{H^k}{k!} \left[\frac{d^k x(t)}{dt^k} \right]_{t=0} \tag{63}$$

$x(k)$ Express the transformed function and $x(t)$ is the original function. The differential spectrum of $x(k)$ is confined within the interval $t \in [0, H]$, where H is a constant. The differential inverse transform of $x(k)$ can be written as follows:

$$x(t) = \sum_{k=0}^{\infty} \left(\frac{t}{H}\right)^k x(k) \tag{64}$$

The values of function $x(k)$ at values of argument k are referred to as discrete, i.e., $x(0)$ is known as the zero discrete, $x(1)$ is the first discrete, etc. Also, the value of the main function $x(t)$ is approximated as a finite power series. The more discrete available, the more precise it is possible to restore the unknown function. The function $x(t)$ consists of the T-function $x(k)$, and its value is given by the sum of the T-function with $(t/H)^k$ as its coefficient. In real applications, at the right choice of constant H , the larger values of argument k result that the discrete spectrum reducing rapidly. The function $x(t)$ is expressed by a finite series and equation (64) can be written as:

$$x(t) = \sum_{k=0}^n \left(\frac{t}{H}\right)^k x(k) \tag{65}$$

Some Mathematical operations that are performed by differential transform are listed in Table 1.

DTM Method problem analysis

The dimensionless parameters in this issue are:

$$\theta = \frac{(T - T_{\infty})}{(T_1 - T_{\infty})}, \quad \lambda = \frac{x}{L}, \quad \mu = \left(\frac{\rho h}{EA} L^2\right)^{\frac{1}{2}} \tag{66}$$

According to the differential transform of the equation (48):

$$\frac{d^2\theta}{d\lambda^2} - \mu^2\theta = 0 \tag{67}$$

$$\theta = 1 \text{ at } \lambda = 1, \quad \frac{d\theta}{d\lambda} = 0 \text{ at } \lambda = 0$$

Table 1. Some fundamental operations of the Differential transform method [18]

Original function	Transformed function
$X(t) = \alpha f(x) \pm \beta g(t)$	$X(k) = \alpha F(k) \pm \beta G(k)$
$X(t) = \frac{df(t)}{dt}$	$X(k) = (k+1)F(k+1)$
$X(t) = \frac{d^2f(t)}{dt^2}$	$X(k) = (k+1)(k+2)F(k+1)$
$X(t) = \exp(t)$	$X(k) = \frac{k}{k!}$
$X(t) = f(t)g(t)$	$X(k) = \sum_{l=0}^k F(l)G(k-l)$

Boundary condition transformed form is:

$$\theta_0 = a \tag{68}$$

The other boundary conditions are considered as follows:

$$\theta_1 = 0 \tag{69}$$

Now we apply DTM from Table 1 into equation (67), we have:

$$(K + 1)(K + 2)\theta(K + 2) - \mu^2\theta(K) = 0 \tag{70}$$

Where a , is constant, and we will calculate it by considering another boundary condition in equation (70) in point $\lambda=1$.

$$\begin{aligned} \theta_2 &= \frac{1}{2}\mu^2a \\ \theta_3 &= 0 \\ \theta_4 &= \frac{1}{24}\mu^4a \\ \theta_5 &= 0 \\ \theta_6 &= \frac{1}{720}\mu^6a \\ \theta_7 &= 0 \\ \theta_8 &= \frac{1}{40320}\mu^8a \\ \theta_9 &= 0 \\ \theta_{10} &= \frac{1}{3628800}\mu^{10}a \\ \theta_{11} &= 0 \\ \theta_{12} &= \frac{1}{479001600}\mu^{12}a \\ \theta_{13} &= 0 \\ \theta_{14} &= \frac{1}{87178291200}\mu^{14}a \\ \theta_{15} &= 0 \\ \theta_{16} &= \frac{1}{20922789888000}\mu^{16}a \\ \theta_{17} &= 0 \\ \theta_{18} &= \frac{1}{6402373705728000}\mu^{18}a \end{aligned} \tag{71}$$

To obtain the value of a , we substitute the boundary condition from Eq. (70) into equation (71) in point $\lambda=1$, and we can be written as:

$$\begin{aligned} \theta(\lambda) &= a + \frac{1}{2}\mu^2a + \frac{1}{24}\mu^4a + \frac{1}{720}\mu^6a \\ &+ \frac{1}{40320}\mu^8a + \frac{1}{3628800}\mu^{10}a \\ &+ \frac{1}{479001600}\mu^{12}a \\ &+ \frac{1}{87178291200}\mu^{14}a \\ &+ \frac{1}{20922789888000}\mu^{16}a \\ &+ \frac{1}{6402373705728000}\mu^{18}a \end{aligned} \tag{72}$$

Now we apply DTM from Table 1 into equation (70) for find temperature distribution will be obtained as:

$$\begin{aligned} \theta(1) = & a + \frac{1}{2}\mu^2 a + \frac{1}{24}\mu^4 a + \frac{1}{720}\mu^6 a \\ & + \frac{1}{40320}\mu^8 a + \frac{1}{3628800}\mu^{10} a \\ & + \frac{1}{479001600}\mu^{12} a \\ & + \frac{1}{87178291200}\mu^{14} a \\ & + \frac{1}{20922789888000}\mu^{16} a \\ & + \frac{1}{6402373705728000}\mu^{18} a = 1 \end{aligned} \tag{73}$$

Solving equation (73), gives the value of a. To calculate $\theta(\lambda)$, it is enough to substitute obtained a in equation (72).

5. Finite element formulation

A rectangular Kevlar/epoxy composite plate was simulated using the finite element software ABAQUS Standard 6.13.1. The length of this rectangular laminate was $L=0.40125$ m and the width of this rectangular laminate was $w = 0.25$ m. The thickness of rectangular Kevlar/epoxy laminate was 0.0025 m. Table 2 lists the different numerical examples. Rectangular Kevlar/epoxy laminate was modeled using heat transfer quadrilateral elements, with three elements along the rectangular examined. All the elements had a size of 0.01 m. Table 3 displays the mechanical Properties of the composite laminate. Figure 5 shows a schematic of the geometry of the problem in question and Fig. 6 shows a rectangular fin. By validating the results in one composite layer, the temperature distribution in several composite layers was finally simulated in ABAQUS software. Table 1 shows the geometry and boundary conditions in the problem Also, the values of density and specific heat capacity are respectively $935 \frac{\text{J kg}}{\text{K}}$ and $1400 \frac{\text{kg}}{\text{m}^3}$ [38]. The fiber angle in all layers is equal to zero. The compound material intended for this part of the composition (25% epoxy with 75% graphite fibers Kevlar/epoxy) [38].

Table 2. problem geometry and boundary condition

$L(m)$	T_l	T_∞	$(\frac{w}{m^2K})$
0.40125	320	300	0.0053,0.021 0.086,0.344,2.15

Table 3. Mechanical properties of composite laminate

material	Density ($\frac{\text{kg}}{\text{m}^3}$)	Specific heat ($\frac{\text{J}}{\text{kg K}}$)	thermal conductivity in the direction of fibers ($\frac{\text{w}}{\text{m K}}$)	thermal conductivity in the direction perpendicular to the fibers ($\frac{\text{w}}{\text{m K}}$)
Kevlar epoxy	1400	935	11.1	0.87

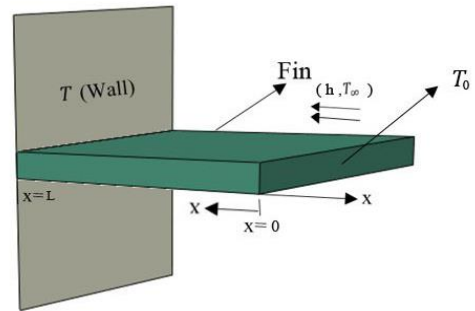


Fig. 5. Schematic of a rectangular composite fin

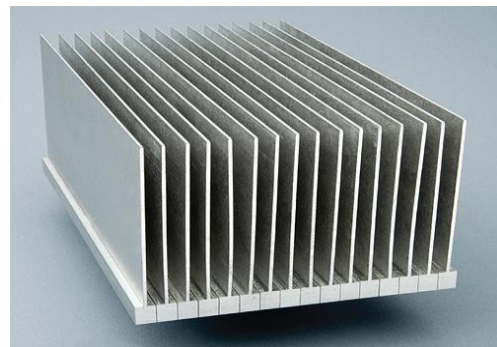


Fig. 6. Industrial samples of rectangular fin

6. Results and discussion

6.1. Case 1

In this study, the heat transfer of a rectangular fin has been investigated by three different methods. The exact solution, DTM, and FEM are used for solving the current problem. The angle of the fibers in all layers should be 0° . In this case, all the fibers are in the X-direction. Boundary conditions applied in this paper, a boundary condition of constant temperature, and the insulated tip boundary condition. The surface of the fin is exposed to fluid flow. A very interesting agreement between the results is observed, which confirms the validity of the DTM and FEM. Figure 7 displays an example of the comparison of the temperature distribution in DTM, FEM, and exact results. The FEM results are in good agreement with the DTM and analytical results. The difference between the FEM results with DTM and analytical results is about 0.25%. Figures 8-10 show the dimensionless variable for temperature distribution with various values of thermo-geometric fin parameter (μ) from 0.25 to

5 in the exact solution, DTM, and FEM. The results depict that DTM and FEM are very useful methods to solve this problem. The trend of change in all results is quite similar and this minor difference can be ignored.

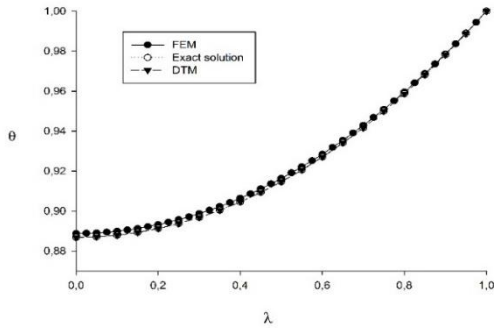


Fig. 7. Example of the comparison of the solutions between DTM, FEM and exact results in $\mu=0.5$

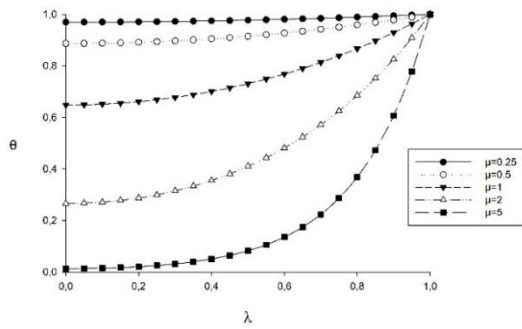


Fig. 8. dimensionless variable for temperature distribution in the exact solution

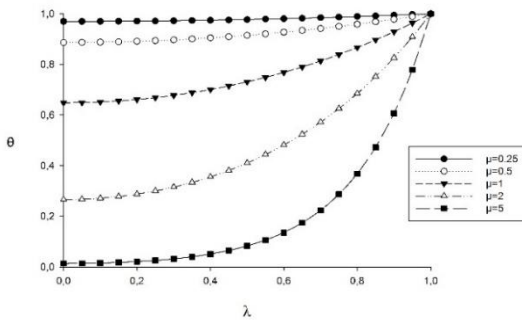


Fig. 9. dimensionless variable for temperature distribution in DTM

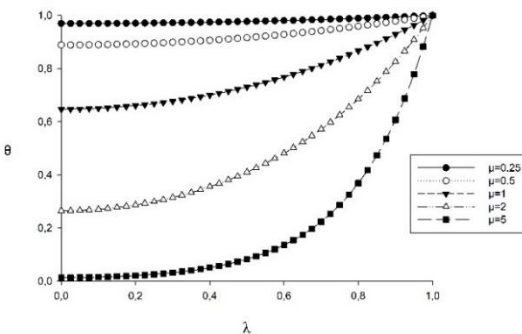


Fig. 10. Dimensionless variable for temperature distribution in FEM

The thermo- Geometric fin parameter (μ) has a significant effect on the dimensionless variable for temperature distribution. By increasing the thermo-geometric fin parameter (μ) the heat transfer becomes further. This is due to the increase in heat transfer rate is between the blade and the environment. Figure 11 displays heat flux distribution versus λ at various thermo-geometric fin parameter (μ) from 0.25 to 5 in FEM. When the thermal conductivity coefficient increases the thermo-geometric fin parameter (μ) increases. By increasing the thermo-geometric fin parameter (μ) heat transfer rate from the fin increase. Finally, The heat flux between composite fin and fluid increases. Also, these changes are more μ coefficients is possible. The results reveal heat flux in $\mu = 0.25$ is negligible and value of about 33 w but by increasing the thermo-geometric fin parameter (μ), in $\mu = 5$ its maximum value is about 2.6 kW. Figure 12 shows heat flux distribution with the temperature distribution with various values of thermo-geometric fin parameter (μ) from 0.25 to 5 in FEM. it can be concluded that by increasing the thermo-geometric fin parameter (μ), the temperature changes increase. With increasing temperature changes along the fin, the heat transfer between the fin and the environment increases. With increasing heat transfer, we will see an increase in heat flux. According to the analysis and accuracy of the DTM solution and exact solution, the results obtained can be used as a criterion for measuring numerical solutions approximate search.

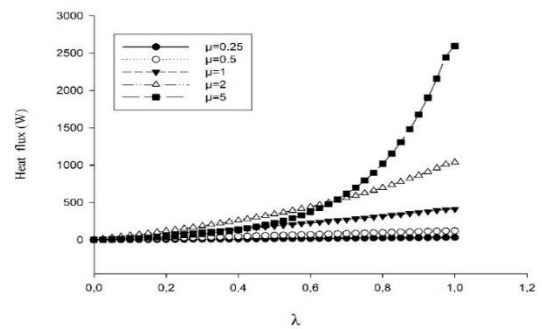


Fig. 11. Heat flux distribution in FEM

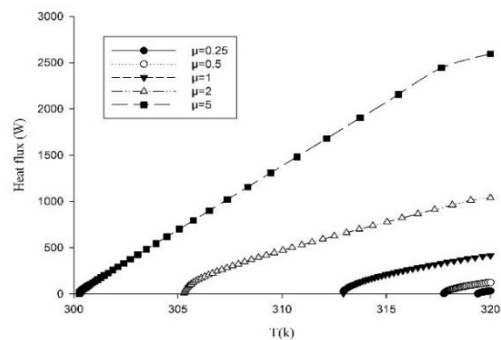


Fig. 12. Heat flux distribution with temperature distribution in FEM

6.2. Case 2

In this case, we studied the effect of the number of composite layers on temperature distribution and the heat flux of the rectangular composite laminate. Figure 13 shows the fibers direction in two and three layers of composite fins. All the fibers are in the X-direction. The angle of the fibers in all layers should be 0° . The thickness of all layers was equal and its value is 0.0025 m.

Figure 14 shows the dimensionless variable for temperature distribution with different numbers of composite layers from 1 to 3 layers. The results display that when the number of composite layers increases, the temperature distribution decrease along the fin. By increasing the number of layers from one layer to two layers, temperature changes are significant and decrease by about 6%. By increasing the number of composite layers from two layers to three layers, temperature changes are relatively small and about 2%. The results show that increasing the layers up to a certain number is justified. But after a certain number, with increasing the number of composite layers, there is not much change in the temperature distribution along the fin.

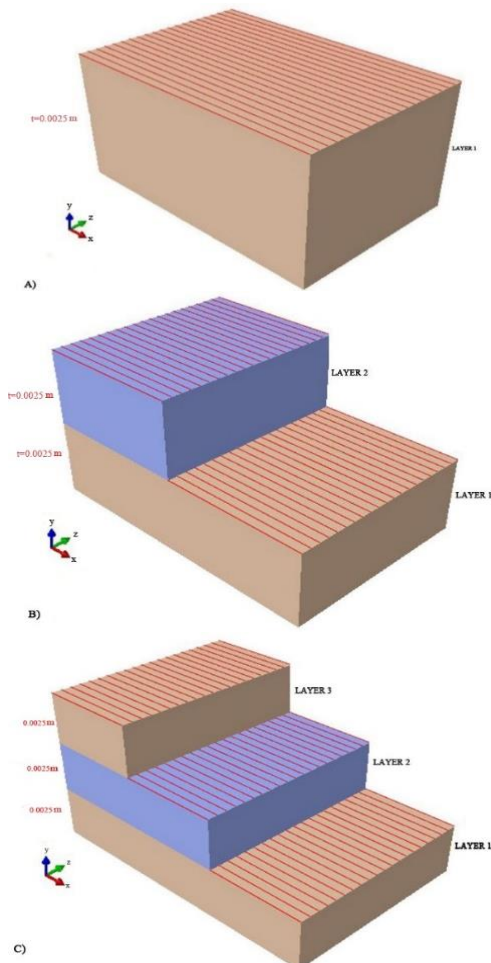


Fig. 13. The fibers' direction in A) one layer, B) two layers, and C) three layers composite fin

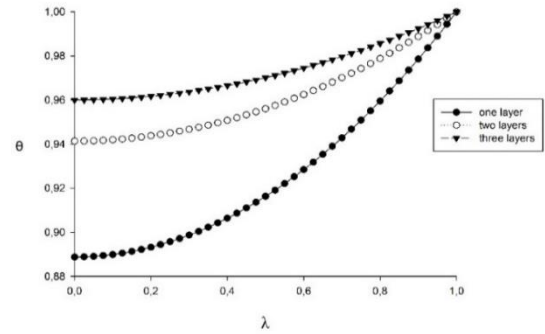


Fig. 14. Dimensionless variable for temperature distribution with different number of composite layers in FEM

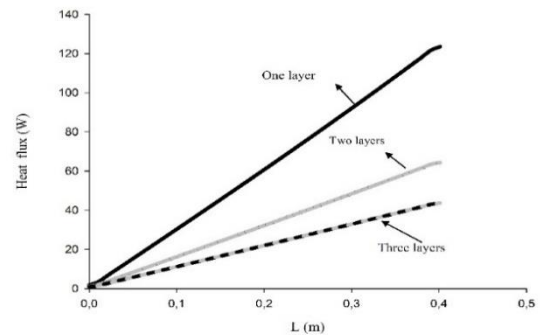


Fig. 15. Heat flux distribution with different numbers of composite layers in FEM

Figure 15 shows the heat flux with different numbers of composite layers from 1 to 3 layers. The results depict that when the number of layers increases, heat flux decrease along the fin. The result displays that when the number of layers increases, heat transfer occurs at a lower rate than single-layer composite and multilayer composite materials have more insulating behavior with rectangular geometry. By increasing the number of composite layers from one layer to two layers, heat flux is significant and decreases by about 47%. By increasing the number of layers from two layers to three layers, heat flux is relatively small and about 32% compared to the two layers. The results show that by increasing the number of layers to a certain number, the changes will be closer to each other and will not be much different from each other. Therefore, in this study, the maximum number of layers was considered three layers.

6.3. Case 3

Considering the comparison of the FEM results in the steady state with the analytical solution and DTM in this section, it has been tried to show the ability to solve and investigate the problems related to multilayer composite in the unsteady by providing a practical example. In this case, we studied the heat flux and temperature distribution of the rectangular composite fins in unsteady heat transfer. The angle of the fibers in all layers should be 0° . In this case, all the fibers are in the X direction and time values (t) were

from 10 s to 600 s in FEM. Figure 16 displays temperature distribution and unsteady heat transfer in rectangular composite fins. According to the results of Fig. 16, it can be concluded that the temperature changes in 10 s along the fin length a large slope. With an increasing time of 600 s, the rate of heat transfer from the blade increases, and the slope of the graph decreases. Finally, the temperature distribution diagram becomes more uniform along the fin.

Figure 17 shows the heat flux in unsteady heat transfer in rectangular composite fins. The results depict that with increasing time the heat flux becomes more uniform and the ratio of heat flux changes decreases along the fin. At 10 s the maximum heat flux value is about 13.3 kW and with increasing time at 600 s this value decreases to about 2.9 kW. The results show that with increasing time up to 100 s, the heat flux changes are significant and its value is about 65%. In the range of 100 s to 600 s these changes it becomes more uniform and its slope decreases and its value is about 78%. The choice of this time range is only to investigate the unsteady analysis of heat transfer in composite fins, and according to various issues, the ideal time range of the problem can be examined.

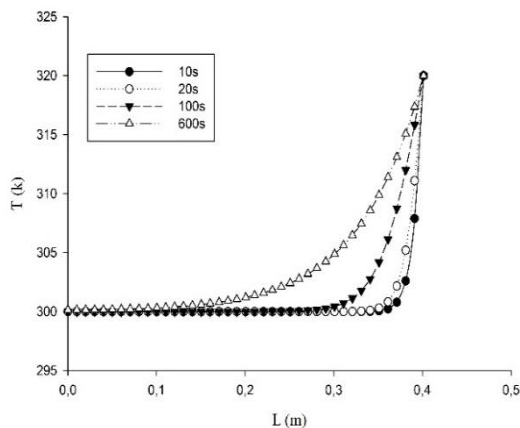


Fig. 16. Effect of time on temperature distribution in FEM

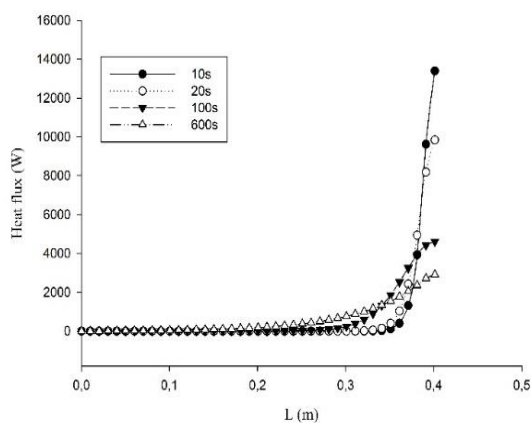


Fig. 17. Effect of time on heat flux distribution in FEM

7. Conclusion

This paper presents an exact, Differential Transform Method and numerical solution for steady-state conduction heat transfer in rectangular composite laminates. The differential Transformation Method (DTM), is applied for predicting the temperature distribution in a rectangular composite fin.

1. The figures and tables clearly show the high accuracy of DTM to solve heat transfer problems in engineering. By comparing the simulation results with the exact solution and DTM results. The results obtained can be used as a criterion for measuring numerical solutions approximate search.
2. The thermo-geometric fin parameter (μ) has a significant effect on the dimensionless variable for temperature distribution by increasing the thermo-geometric fin parameter (μ) the heat transfer becomes further.
3. The thermo-geometric fin parameter (μ) has a significant effect on heat flux change. When $\mu = 0.25$, the heat flux between composite fin and fluid is very low but by increasing of thermo-geometric fin parameter (μ) to $\mu = 5$, the heat flux between composite fin and fluid is increased.
4. The number of composite layers has a significant effect on the changes in the dimensionless variable for temperature and thermal flux. The results show when the number of layers increases, the dimensionless variable for temperature distribution and heat flux decrease along the fin. By increasing the number of layers to a certain number, the changes will be closer to each other and will not be much different from each other. Therefore, in this study, the maximum number of layers was considered three layers.
5. With an increasing time of 600s, the rate of heat transfer from the blade increases, and the slope of the graph decreases. The temperature distribution diagram becomes more uniform along the fin.
6. The results depict that with increasing time the heat flux becomes more uniform and the ratio of heat flux changes decreases along the fin. Which is significant in 10s and decreases with increasing time to 600s.

Nomenclature

k_{ij}	Main thermal conductivity coefficients (w/mk)
\overline{k}_{ij}	Subsidiary thermal conductivity coefficients (w/mk)
(X_1, X_2, X_3)	Main axis coordinate systems
(X, Y, Z)	Subsidiary axis coordinate systems
Q	Heat flux (W)
T	Temperature
θ	Rotation tensor transform
k_f	Fiber thermal conductivity coefficient
k_m	The Thermal conductivity coefficient of background material
v_f	Volumetric percentage of fiber
v_m	Volume percentage of background material
C	Specific heat capacity
ρ	Density
V	Volume
I	Number of layer
H	External heat transfer coefficient (w/(m ² K))
p	Rectangular fin perimeter (m)
A	Cross-sectional area of the fin (m ²)
θ	Dimensionless variable for temperature difference
$x(k)$	Express the transformed function For The McLaurin series
$x(t)$	Original function For The McLaurin series
Λ	Dimensionless coordinate
μ	Thermo-geometric fin parameter
T_L	Temperature of $x=L$ (K)
a,b	Arbitrary coefficients of the equation (58)
t	Thickness of laminate(mm)

References

- [1] A. Vestergaard, S. J. Hansen and H.T. Denning, 1998. Valve, In Particular Expansion Valve for Refrigeration Stems Thereof, *United States Patent*, Assignee: DanfossAJS, Nordborg, Denmark Patent Number 45, US5810332.
- [2] W. A. Wooster, 1957. A textbook in crystal physics. *Cambridge University Press*, London, textbook p. 455.
- [3] M.N. Ozisik. 1993. Heat conduction. *Wiley*, New York.
- [4] J. Argyris, L. Tenek, F. Oberg, 1995. A Multilayer Composite Triangular Element for Steady-State Conduction/Convection/Radiation Heat Transfer in Complex Shells, *Comput. Methods Appl.Mech. Eng*, Vol. 120, pp. 271-301.
- [5] M. H. Hsieh, C. C. Ma, 2002. Analytical Investigations for Heat Conduction Problems in Anisotropic Thin-Layer Media with Embedded Heat Sources, *Int. J. Heat and Mass Transfer*, Vol. 45, No. 20, pp. 4117-4132.
- [6] C. C. Ma, S. W. Chang, 2004. Analytical Exact Solutions of Heat Conduction Problems for Anisotropic Multilayered Media, *Int. J. Heat and Mass Transfer*, Vol. 47, No. 9, pp. 1643-1655.
- [7] T. Guo, 2004. Temperature Distribution of Thick Thermo Set Composites, *J. Model. Simul. Mater.Sci. Eng*, Vol. 12, No. 2, pp. 443-452.
- [8] C. Corlay, S. G. Advani, 2007. Temperature Distribution in a Thin Composite Plate Exposed to a Concentrated Heat Source, *Int. J. Heat and Mass Transfer*, Vol. 50 No. 4, pp. 2883-2894.
- [9] B. Yazicioglu, H. Yuncu, 2007. Optimum fin spacing of rectangular fins on a vertical base in free convection heat transfer, *Journal of heat and mass transfer*, vol. 44, no. 1, pp. 11-21.
- [10] L. Dialameh, M. Yaghoubi, O. Abouali, 2008. Natural convection from an array of horizontal rectangular thick fins with short length, *Appl. Thermal Eng.* 28, 2371-2379.
- [11] A.A. Joneidi, D.D. Ganji, M. Babaelahi, 2009. Differential Transformation Method to determine fin efficiency of convective straight fins with temperature dependent thermal conductivity, *International Communications in Heat and Mass Transfer*, 757-762, 36.
- [12] S. V. Naidu, V. Dharma Rao, 2010. Natural convection heat transfer from fin arrays experimental and theoretical study on effect of inclination of base on heat transfer, *ARPN Journal of Engineering and Applied Sciences*, Vol. 5, No. 9, Sept.
- [13] Y. Tanigawa, Y. Ootao., R. Kawamura, 2013. thermal bending analysis of a laminated composite rectangular plate due to a partially distributed heat supply, *Journal of Thermal Stresses*, pp. 37-41.
- [14] I. Tari, M. Mehrtash, 2013. Natural convection heat transfer from inclined plate-fin heat sinks, *International Journal of Heat and Mass Transfer* 56,574-593.
- [15] M. Hatami, A. Hasanpour, D.D. Ganji, 2013. Heat transfer study through porous fins (Si3N4 and AL) with temperature-dependent heat generation, *International Communications in Energy Conversion and Management*, 9-1674.

- [16] M. Ahmadi, G. Mostafavi, 2014. Natural convection from rectangular interrupted fins, *International Journal of Thermal Sciences* vol. 82, pp.62-71.
- [17] A. Jacob, G. Chandrashekhara, J. George, J. George, Study, 2015. Design and Optimization of Triangular Fins. *International Journal for Innovative Research in Science & Technology*, Volume 1, Issue 12, ISSN (online), 2349-6010.
- [18] F. Bunjaku, V. Filkoski, N. Sahiti, 2017. Thermal Optimization and Comparison of Geometric Parameters Of Rectangular and Triangular Fins with Constant Surfacing. *Journal of Mechanical Engineering* 63, 7-8, 439-446.
- [19] S. Gupta, S. Singh, 2017. Analytical Thermal Analysis on Straight Triangular Fins, *International Journal of Scientific & Engineering Research* Volume 8, Issue 12, ISSN 2229-5518.
- [20] N. Fallo, R.J. Moitsheki, O.D. Makinde, 2018. Analysis of Heat Transfer in a Cylindrical Spine Fin with Variable Thermal Properties, *University of Technology, Göteborg, Sweden, Trans Tech Publications*.
- [21] N. Namdari, M. Abdi H. Chaghomi, F. Rahmani, 2018. Numerical Solution for Transient Heat Transfer in Longitudinal Fins, *International Research Journal of Advanced Engineering and Scienc*, ISSN (Online): 2455-9024.
- [22] A.V. Pasha, P. Jalili, D.D. Ganji, 2018. Analysis of unsteady heat transfer of specific longitudinal fins with Temperature-dependent thermal coefficients by DTM, *Alexandria Engineering Journal*, Volume 57, Issue 4, Pages 3509-3521.
- [23] H.A. Patel, V.S. Kale, S.U. Joshi, S. D. Jadhav, S.N. Teli, 2019. Comparative Thermal Analysis of Fins, *Proceedings of International Conference on Intelligent Manufacturing and Automation*, Lecture Notes in Mechanical Engineering.
- [24] A.R. Mazhar, A. Shukla S. Liu, 2020. Numerical analysis of rectangular fins in a PCM for low-grade heat harnessing, *International Journal of Thermal Sciences*, Volume 152, 106306.
- [25] R.C. Adhikari, D.H. Wood, M. Pahlevani, 2020. An experimental and numerical study of forced convection heat transfer from rectangular fins at low Reynolds numbers, *International Journal of Heat and Mass Transfer*, Volume 163.
- [26] M.N. Ozisik, 1993. Heat Conduction, Second Ed., New York, Wiley.
- [27] C.T. Herakovich, 1998. Mechanics of Fibrous Composites, New York, *John Wiley and Sons*, INC, 460.
- [28] Y.C. Fung, 1965. Foundation of solid mechanics. *Prentice-Hall*, Englewood Cliffs.
- [29] J.M. Powers, 2004. On the necessity of positive semi-definite conductivity and Onsager reciprocity in modeling heat conduction in anisotropic media. *J Heat Transf Trans Asme* 126(5):670-675.
- [30] J.C. Halpin, 1992. Primer on Composite Materials Analysis, *CRC Press*, 229.
- [31] N. Hassan, J. E. Thompson, R.C. Batra, A.B. Hulcher, X. Song, A.C. Loos, 2005. A Heat Transfer Analysis of the Fiber Placement Composite Manufacturing Process, *Journal of Reinforced Plastic and Composites*, Vol. 24, No. 8 pp. 869-888.
- [32] H.S. Carslaw, J.C. Jaeger, 1971. Conduction of Heat in Solids, London, *Oxford University Press*, 510.
- [33] C.T. Herakovich, 1998. Mechanics of Fibrous Composites, New York, *John Wiley and Sons*, INC, 460.
- [34] J.C. Halpin, 1992. Primer on Composite Materials Analysis, *CRC Press*, 229.
- [35] H.S. Carslaw, J.C. Jaeger, 1971. Conduction of Heat in Solids, London, *Oxford University Press*. 510.
- [36] V.S. Arpaci, 1966. Conduction Heat Transfer, USA, *Addison-Wesley publishing Company*. 550.
- [37] S. Ghafoori, M. Motevalli, M.G. Nejad, F Shakeri, D.D. Ganji, M. Jalaal, 2011. Efficiency of differential transformation method for nonlinear oscillation: comparison with HPM and VIM. *Curr Appl Phys*. 1, 965-71.
- [38] C. Arslanturk, 2005. A decomposition method for fin efficiency of convective straight fins with temperature-dependent thermal conductivity, *Int. Commun. Heat Mass Transfer*, 32, 831-841.
- [39] M. H. Kayhani, M. Norouzi, A. A. Delouei, 2011. Analytical Investigation of Orthotropic Unsteady Heat Transfer in Composite Pin Fins. *Modares Mechanical Engineering*, 11(4):21-32.
- [40] J. H. Lienhard, 1981. a Heat Transfer Textbook, *Prentice-Hall publishers*.